CERN-PPE 90-176
23 November 1990

EUROPEAN ORGANIZATION FOR NUCLEAR RESEARCH

Measurement of the Strong Coupling Constant α_s from Global Event-Shape Variables of Hadronic Z Decays

The ALEPH Collaboration

Abstract

An analysis of global event-shape variables has been carried out for the reaction $e^+e^- \to Z^0 \to$ hadrons to measure the strong coupling constant α_s. This study is based on 52720 hadronic events obtained in 1989/90 with the ALEPH detector at the LEP collider at energies near the peak of the Z-resonance. In order to determine α_s, second order QCD predictions modified by effects of perturbative higher orders and hadronization were fitted to the experimental distributions of event-shape variables. From a detailed analysis of the theoretical uncertainties we find that this approach is best justified for the differential 2-jet rate, from which we obtain $\alpha_s(M_Z^2) = 0.121 \pm 0.002(stat.) \pm 0.003(sys.) \pm 0.007(theo.)$ using a renormalization scale $\mu = M_Z/2$. The dependence of $\alpha_s(M_Z^2)$ on μ is parameterized. For scales $m_b < \mu < M_Z$ the result varies by $^{+0.007}_{-0.012}$.

Submitted to Physics Letters B

The ALEPH Collaboration

D. Decamp, B. Deschizeaux, C. Goy, J.-P. Lees, M.-N. Minard

Laboratoire de Physique des Particules (LAPP), IN²P³-CNRS, 74019 Annecy-le-Vieux Cedex, France

R. Alemany, J.M. Crespo, M. Delfino, E. Fernandez, V. Gaitan, Ll. Garrido, P. Mato, R. Miquel, Ll.M. Mir, S. Orteu, A. Pacheco, J.A. Perlas, E. Tubau

Laboratorio de Fisica de Altas Energias, Universidad Autonoma de Barcelona, 08193 Bellaterra (Barcelona), Spain[9]

M.G. Catanesi, D. Creanza, M. de Palma, A. Farilla, G. Iaselli,[1] G. Maggi, M. Maggi, S. Natali, S. Nuzzo, M. Quattromini, A. Ranieri, G. Raso, F. Romano, F. Ruggieri, G. Selvaggi, L. Silvestris, P. Tempesta, G. Zito

INFN Sezione di Bari e Dipartimento di Fisica dell' Università, 70126 Bari, Italy

Y. Gao, H. Hu,[22] D. Huang, X. Huang, J. Lin, J. Lou, C. Qiao,[22] T. Ruan,[22] Wang, Y. Xie, D. Xu, R. Xu, J. Zhang, W. Zhao

Institute of High-Energy Physics, Academia Sinica, Beijing, The People's Republic of China[10]

H. Albrecht,[2] W.B. Atwood,[3] F. Bird, E. Blucher, G. Bonvicini, F. Bossi, J. Bourotte, D. Brown, T.H. Burnett,[4] H. Drevermann, F. Dydak, R.W. Forty, C. Grab, R. Hagelberg, S. Haywood, B. Jost, M. Kasemann, G. Kellner, J. Knobloch, A. Lacourt, I. Lehraus, T. Lohse, D. Lüke,[2] A. Marchioro, M. Martinez, J. May,[2] S. Menary, A. Minten, A. Miotto, J. Nash, P. Palazzi, F. Ranjard, G. Redlinger, A. Roth, J. Rothberg,[4] H. Rotscheidt, W. von Rüden, R. St.Denis, D. Schlatter, M. Takashima, M. Talby,[5] W. Tejessy, H. Wachsmuth, S. Wasserbaech, S. Wheeler, W. Wiedenmann, W. Witzeling, J. Wotschack

European Laboratory for Particle Physics (CERN), 1211 Geneva 23, Switzerland

Z. Ajaltouni, M. Bardadin-Otwinowska, A. Falvard, R. El Fellous, P. Gay, P. Henrard, J. Jousset, B. Michel, J-C. Montret, D. Pallin, P. Perret, J. Proriol, F. Prulhière

Laboratoire de Physique Corpusculaire, Université Blaise Pascal, IN²P³-CNRS, Clermont-Ferrand, 63177 Aubière, France

J.D. Hansen, J.R. Hansen, P.H. Hansen, R. Møllerud, E.R. Nielsen, B.S. Nilsson, G. Petersen

Niels Bohr Institute, 2100 Copenhagen, Denmark[11]

I. Efthymiopoulos, E. Simopoulou, A. Vayaki

Nuclear Research Center Demokritos (NRCD), Athens, Greece

J. Badier, A. Blondel, G. Bonneaud, F. Braems, J.C. Brient, G. Fouque, A. Gamess, R. Guirlet, A. Rosowsky, A. Rougé, M. Rumpf, R. Tanaka, H. Videau, I. Videau

Laboratoire de Physique Nucléaire et des Hautes Energies, Ecole Polytechnique, IN²P³-CNRS, 91128 Palaiseau Cedex, France

D.J. Candlin

Department of Physics, University of Edinburgh, Edinburgh EH9 3JZ, United Kingdom[12]

G. Parrini

Dipartimento di Fisica, Università di Firenze, INFN Sezione di Firenze, 50125 Firenze, Italy

M. Corden, C. Georgiopoulos, M. Ikeda, J. Lannutti, D. Levinthal,[17] M. Mermikides, L. Sawyer, G. Stimpfl

Supercomputer Computations Research Institute and Dept. of Physics, Florida State University, Tallahassee, FL 32306, USA[14,15,16]

A. Antonelli, R. Baldini, G. Bencivenni, G. Bologna,[6] P. Campana, G. Capon, V. Chiarella, B. D'Ettorre-Piazzoli,[7] G. Felici, P. Laurelli, G. Mannocchi,[7] F. Massimo-Brancacci, F. Murtas, G.P. Murtas, G. Nicoletti, L. Passalacqua, M. Pepe-Altarelli, P. Picchi,[6] P. Zografou

Laboratori Nazionali dell'INFN (LNF-INFN), 00044 Frascati, Italy

B. Altoon, O. Boyle, A.W. Halley, I. ten Have, J.L. Hearns, J.G. Lynch, W.T. Morton, C. Raine, J.M. Scarr, K. Smith, A.S. Thompson, R.M. Turnbull

Department of Physics and Astronomy, University of Glasgow, Glasgow G12 8QQ, United Kingdom[12]

B. Brandl, O. Braun, R. Geiges, C. Geweniger, P. Hanke, V. Hepp, E.E. Kluge, Y. Maumary, A. Putzer, B. Rensch, A. Stahl, K. Tittel, M. Wunsch

Institut für Hochenergiephysik, Universität Heidelberg, 6900 Heidelberg, Fed. Rep. of Germany[18]

A.T. Belk, R. Beuselinck, D.M. Binnie, W. Cameron, M. Cattaneo, P.J. Dornan, S. Dugeay, A.M. Greene, J.F. Hassard, S.J. Patton, J.K. Sedgbeer, G. Taylor, I.R. Tomalin, A.G. Wright

Department of Physics, Imperial College, London SW7 2BZ, United Kingdom[12]

P. Girtler, D. Kuhn, G. Rudolph

Institut für Experimentalphysik, Universität Innsbruck, 6020 Innsbruck, Austria[20]

C.K. Bowdery[1], T.J. Brodbeck, A.J. Finch, F. Foster, G. Hughes, N.R. Keemer, M. Nuttall, B.S. Rowlingson, T. Sloan, S.W. Snow

Department of Physics, University of Lancaster, Lancaster LA1 4YB, United Kingdom[12]

T. Barczewski, L.A.T. Bauerdick, K. Kleinknecht, B. Renk, S. Roehn, H.-G. Sander, M. Schmelling, H. Schmidt, F. Steeg

Institut für Physik, Universität Mainz, 6500 Mainz, Fed. Rep. of Germany[18]

J-P. Albanese, J-J. Aubert, C. Benchouk, V. Bernard, A. Bonissent, D. Courvoisier, F. Etienne, S. Papalexiou, P. Payre, B. Pietrzyk, Z. Qian

Centre de Physique des Particules, Faculté des Sciences de Luminy, IN^{2}P^3-CNRS, 13288 Marseille, France

W. Blum, P. Cattaneo, G. Cowan, B. Dehning, H. Dietl, M. Fernandez-Bosman, T. Hansl-Kozanecka[23], G. Hauser, A. Jahn, W. Kozanecki,[3,24] E. Lange, G. Lütjens, G. Lutz, W. Männer, H-G. Moser, Y. Pan, R. Richter, A.S. Schwarz, R. Settles, U. Stierlin, J. Thomas, G. Wolf

Max-Planck-Institut für Physik und Astrophysik, Werner-Heisenberg-Institut für Physik, 8000 München, Fed. Rep. of Germany[18]

V. Bertin, G. de Bouard, J. Boucrot, O. Callot[1], X. Chen, A. Cordier, M. Davier, G. Ganis, J.-F. Grivaz, Ph. Heusse, P. Janot, V. Journé, D.W. Kim[21], J. Lefrançois, A.-M. Lutz, J.-J. Veillet, Z. Zhang, F. Zomer

Laboratoire de l'Accéléateur Linéaire, Université de Paris-Sud, IN^{2}P^3-CNRS, 91405 Orsay Cedex, France

S.R. Amendolia, G. Bagliesi, G. Batignani, L. Bosisio, U. Bottigli, C. Bradaschia, M.A. Ciocci, I. Ferrante, F. Fidecaro, L. Foà[1], E. Focardi, F. Forti, A. Giassi, M.A. Giorgi, F. Ligabue, A. Lusiani, E.B. Mannelli, P.S. Marrocchesi, A. Messineo, L. Moneta, F. Palla, G. Sanguinetti, J. Steinberger, R. Tenchini, G. Tonelli, G. Triggiani, A. Venturi, J. Walsh

Dipartimento di Fisica dell'Università, INFN Sezione di Pisa, e Scuola Normale Superiore, 56010 Pisa, Italy

J.M. Carter, M.G. Green, P.V. March, T. Medcalf, M.R. Saich, J.A. Strong, R.M. Thomas, T. Wildish

Department of Physics, Royal Holloway & Bedford New College, University of London, Surrey TW20 OEX, United Kingdom[12]

D.R. Botterill, R.W. Clifft, T.R. Edgecock, M. Edwards, S.M. Fisher, J. Harvey, T.J. Jones, P.R. Norton, D.P. Salmon, J.C. Thompson

Particle Physics Dept., Rutherford Appleton Laboratory, Chilton, Didcot, OXON OX11 OQX, United Kingdom[12]

B. Bloch-Devaux, P. Colas, C. Klopfenstein, E. Lançon, E. Locci, S. Loucatos, L. Mirabito, E. Monnier, P. Perez, F. Perrier, J. Rander, J.-F. Renardy, A. Roussarie, J.-P. Schuller, J. Schwindling

Département de Physique des Particules Élémentaires, CEN-Saclay, 91191 Gif-sur-Yvette Cedex, France[19]

J.G. Ashman, C.N. Booth, C. Buttar, R. Carney, S. Cartwright, F. Combley, M. Dinsdale, M. Dogru, F. Hatfield, J. Martin, D. Parker, P. Reeves, L.F. Thompson

Department of Physics, University of Sheffield, Sheffield S3 7RH, United Kingdom[12]

S. Brandt, H. Burkhardt, C. Grupen, H. Meinhard, E. Neugebauer, U. Schäfer, H. Seywerd

Fachbereich Physik, Universität Siegen, 5900 Siegen, Fed. Rep. of Germany[18]

G. Apollinari, G. Giannini, B. Gobbo, F. Liello, L. Rolandi, U. Stiegler

Dipartimento di Fisica, Università di Trieste e INFN Sezione di Trieste, 34127 Trieste, Italy

L. Bellantoni, J.F. Boudreau, D. Cinabro, J.S. Conway, D.F. Cowen, A.J. DeWeerd, Z. Feng, D.P.S. Ferguson, Y.S. Gao, J.L. Harton, J. Hilgart, J.E. Jacobsen, R.C. Jared[8], R.P. Johnson, B.W. LeClaire, Y.B. Pan, T. Parker, J.R. Pater, Y. Saadi, V. Sharma, J.A. Wear, F.V. Weber, Sau Lan Wu, G. Zobernig

Department of Physics, University of Wisconsin, Madison, WI 53706, USA[18]

[1] Now at CERN.
[2] Permanent address: DESY, Hamburg, Fed. Rep. of Germany.
[3] On leave of absence from SLAC, Stanford, CA 94309, USA.
[4] On leave of absence from University of Washington, Seattle, WA 98195, USA.
[5] Also Centre de Physique des Particules, Faculté des Sciences, Marseille, France
[6] Also Istituto di Fisica Generale, Università di Torino, Torino, Italy.
[7] Also Istituto di Cosmo-Geofisica del C.N.R., Torino, Italy.
[8] Permanent address: LBL, Berkeley, CA 94720, USA.
[9] Supported by CAICYT, Spain.
[10] Supported by the National Science Foundation of China.
[11] Supported by the Danish Natural Science Research Council.
[12] Supported by the UK Science and Engineering Research Council.
[13] Supported by the US Department of Energy, contract DE-AC02-76ER00881.
[14] Supported by the US Department of Energy, contract DE-FG05-87ER40319.
[15] Supported by the NSF, contract PHY-8451274.
[16] Supported by the US Department of Energy, contract DE-FC0S-85ER250000.
[17] Supported by SLOAN fellowship, contract BR 2703.
[18] Supported by the Bundesministerium für Forschung und Technologie, Fed. Rep. of Germany.
[19] Supported by the Institut de Recherche Fondamentale du C.E.A..
[20] Supported by Fonds zur Förderung der wissenschaftlichen Forschung, Austria.
[21] Supported by the Korean Science and Engineering Foundation and Ministry of Education.
[22] Supported by the World Laboratory.
[23] On leave of absence from MIT, Cambridge, MA02139, USA.
[24] Supported by Alexander von Humboldt Fellowship, Germany.

1. Introduction

We report on a determination of the strong coupling constant, α_s, based on properties of hadronic events from electron-positron annihilation at center-of-mass energies in the range 91.0 GeV $\leq E_{CM} \leq$ 91.5 GeV. Similar studies were done for lower energies at PEP and PETRA [1]. The reaction $e^+e^- \rightarrow$ hadrons is described in the Standard Model as the annihilation of the electron and positron into a gauge boson, which then decays into a quark-antiquark pair. In absence of a complete theoretical description of the transformation of the initial quark-antiquark pair into the final hadrons, this fragmentation process is devided into two steps:

- The subsequent emission of quarks and gluons, described by perturbative QCD.
- The hadronization, where a system of partons is transformed into observable hadrons, described by phenomenological models.

Perturbative QCD calculations to order α_s^2 are available for parton level distributions of several event-shape variables which are insensitive to soft or collinear gluon emission. A comprehensive review is given in reference [2]. The effects of the unknown higher order corrections and the final hadronization process hamper the direct comparison of these theoretical predictions with the data. This is expected to limit the attainable precision of a measurement of α_s to $\approx 10\%$ at LEP energies.

The paper is organized as follows. After a description of event selection and data correction in chapter 2 we describe our analysis strategy in chapter 3. In chapter 4 the model calculations used to estimate the theoretical errors are discussed. In chapter 5 we finally present the results for α_s for a set of global event-shape variables, i.e. variables where the structure of an event is decribed by a single number. Chapter 6 summarizes the result.

2. Data Analysis

A description of the ALEPH detector which provides both tracking information and calorimetry over almost the full solid angle can be found in reference [3].

The trigger used was a total energy trigger requiring at least 6.5 GeV in the barrel of the electromagnetic calorimeter or 3.8 GeV in either endcap or 1.6 GeV in both endcaps. A second trigger was a penetrating particle trigger requiring at least four hits in the hadron calorimeter in an azimuthal region where at least 6 coordinates in the Inner Tracking Chamber (ITC) were recorded. The combined efficiency of both triggers was 100% for hadronic events.

The measurements presented here are based on the charged particles measured by the Time Projection Chamber (TPC) and the ITC of the ALEPH detector. Charged tracks are required to have at least four three-dimensional coordinates from the TPC, to extrapolate to within 2 cm of the beam line and to within 5 cm of the origin in the direction along the beam. In addition, the angle with respect to the beam is required to be at least 20 degrees, and the transverse momentum component relative to the beam must be at least 200 MeV/c. Using tracks which meet these criteria, the sphericity axis and the total charged energy are computed. Events are required to have at least five accepted charged tracks, the polar angle of the sphericity axis, θ_{sph}, in the range $35^\circ \leq \theta_{sph} \leq 145^\circ$, and a total charged energy of at least 15 GeV.

We have measured the global event-shape variables Thrust, Oblateness, C-parameter, Heavy Jet Mass, Mass Difference and Differential Two-Jet Rate. The C-parameter is defined by $C = 3(\lambda_1\lambda_2 + \lambda_2\lambda_3 + \lambda_3\lambda_1)$ with $\lambda_{i=1,2,3}$ the eigenvalues of the spherocity tensor $T_{ij} = (\sum_a (p_a^i p_a^j)/p_a)/\sum_a p_a$. Heavy Jet Mass and Mass Difference are defined by $M_{H,T}^2/s$ and $M_{D,T}^2 = (M_{H,T}^2 - M_{L,T}^2)/s$, with $s = E_{cm}^2$ and $M_{H,T}$ ($M_{L,T}$) the larger (smaller) one of the invariant

masses seen in the two hemispheres defined by the plane orthogonal to the thrust direction. The Differential Two-Jet Rate dn/dy_3, i.e. the distribution of the jet resolution parameter y_3 which marks the transition between two and three jets for a given event was measured with the E_0 clustering algorithm: One starts out by considering each final state particle to be a jet. The resolution parameter $y_{ij} = 2E_iE_j(1-\cos\theta_{ij})/E_{vis}^2$ ("JADE metric"[4]) is determined for any pair of jets i and j and the pair with the smallest value is merged into one jet with energy $E_{ij} = E_i + E_j$ and momentum $\vec{p}_{ij} = (\vec{p}_i + \vec{p}_j) \cdot E_{ij}/|\vec{p}_i + \vec{p}_j|$. The procedure is iterated until only three jets are left at which point the smallest y_{ij} is the value of y_3 for the event.

All event-shape distributions were corrected for effects of geometrical acceptance, detector efficiency and resolution, decays, missing neutral particles, secondary interactions and initial state photon radiation by the following procedure: A first set of hadronic events with flavour composition as predicted by the Standard Model was generated using the Lund Parton-Shower model (PS) [5] including initial state photon radiation. The events were passed through the detector simulation program to produce simulated raw data, which were then processed through the same reconstruction and analysis chain as the real data. A second set of Monte Carlo data without detector simulation was generated, in which all particles with mean lifetimes less than 1 ns were required to decay, the others were treated as stable, and initial state radiation was turned off. Correction factors for each data point were obtained by comparing bin by bin the two Monte Carlo distributions. These factors were used to correct the measurements to a fixed center-of-mass energy and a well defined final state particle composition that can be compared directly to QCD model calculations. For the regions used to extract the strong coupling constant the corrections are typically between 1.0 and 1.25 and dominated by the geometrical acceptance. The correction for neutral particles is typically less than 5%. The experimental systematic errors due to these corrections were estimated by varying the selection cuts and simulating the effects of residual track distortions in the TPC.

3. Determination of $\alpha_s(M_Z^2)$

In the determination of the strong coupling constant α_s the theoretical predictions from a second order QCD calculation [2] based on the Ellis-Ross-Terano (ERT) matrix elements [6] were convoluted with a phenomenological "smearing function" and fit to the experimental distributions. The smearing function $f_x(x_p, x_h)$ is the probability density that an event-shape variable x with the value x_p at the parton level acquires the value x_h in the hadronic final state. Integrating $f_x(x_p, x_h)$ over finite bin sizes yields transition probabilities p_{ij} that an event which at the parton level belongs in bin j falls into bin i after hadronization. Various smearing functions based on different hadronization models [5,7,8] were used, and the spread in the α_s values obtained is taken as an estimate of the theoretical uncertainty.

The correlation between parton and hadron level for y_3 is shown in figure 1 for the Lund second order matrix element model [7]. The gap at low values of y_{3p} is due to the infrared cut-off $y_{min} = 0.01$ (see below). Figure 2(a) shows the ratio of the two projections from figure 1, the dotted lines indicating regions in the event-shape distributions where distortions are small. To illustrate that higher order and hadronization effects can be large the same ratio is displayed in 2(b) for Oblateness. Figures 2(c) and (d) finally show the amount of smearing, i.e. the distribution of $x_p - x_h$, for both variables in the regions between the dotted lines of figs.2(a) and (b). Small width (small smearing distortions) and mean value close to zero (unbiased measurement) for all models are the signature of a "good" event-shape variable, i.e. a variable where the parton level distribution is only slightly distorted by higher order and hadronization

effects. Thus y_3 turns out to be a "good" variable, while oblateness is an example for a "bad" one.

For every event-shape variable, a range in which this variable is least biased and well measured is defined. The regions were required to be sufficiently far from singularities in the partonic cross sections. The y_3 distribution, for example, has its singularity at $y_3 = 0$. Between $y_3 = 0.05$ and $y_3 = 0.30$ the parton level distribution and the hadron level distribution agree within 10%. Above $y_3 = 0.25$, however, the experimental corrections exceed 25%, indicating that the measurement becomes less stable. Therefore, the fit interval was restricted to $0.1 < y_3 < 0.2$. The intervals chosen for all event-shape variables under study are given in table 1.

The strong coupling constant is then obtained by fitting to the data the second order QCD prediction convoluted with the smearing information for the transition from parton to hadron level. The fit consists in minimizing the χ^2:

$$\chi^2 = \sum_i \frac{(d_i - \sum_j p_{ij} t_j(\alpha_s))^2}{(\sigma_i)^2}. \tag{1}$$

Here the d_i denote the measured cross sections with errors σ_i, $t_j(\alpha_s)$ the second order QCD prediction as a function of the strong coupling constant and p_{ij} the transition probabilities as defined above. Tables of the measured cross section can be found in reference [9]. The theoretical prediction for a given event-shape variable can be obtained through integration of the second order QCD matrix elements as described for example in reference [2]. It can be parameterized in the form

$$t_j = \frac{\alpha_s(\mu^2)}{2\pi} \cdot A_j + (\frac{\alpha_s(\mu^2)}{2\pi})^2 \cdot (2\pi b_0 \ln(\frac{\mu^2}{s}) \cdot A_j + B_j) \tag{2}$$

with $b_0 = (33 - 2n_f)/(12\pi)$. Here, $n_f(= 5)$ denotes the number of active flavours and $\sqrt{s}$ is the center of mass energy. The functions A_j and B_j are specific for every event shape variable and contain the full information of the second order matrix elements. The parameter μ denotes the renormalization scale used for the calculation.

For any scale μ we can determine $\alpha_s(\mu^2)$ by comparing (2) to the data and then translate this result into $\alpha_s(M_Z^2)$ using the two-loop expression for the running coupling constant

$$\alpha_s(\mu^2) = \frac{1}{b_0 \ln(\mu^2/\Lambda^2)} \left(1 - \frac{b_1 \ln(\ln(\mu^2/\Lambda^2))}{b_0^2 \ln(\mu^2/\Lambda^2)}\right) \tag{3}$$

with $b_1 = (153 - 19n_f)/(24\pi^2)$. The μ dependence in (3) is such that equation (2) becomes invariant under changes of μ in order α_s^2, i.e. in the finite order in which the perturbative calculation is done. Therefore, the value $\alpha_s(M_Z^2)$ extracted from (3) does not depend on the scale to this order. The choice of μ does, however, enter the result to third order, reflecting our ignorance of higher order corrections. Since α_s is relatively large (as compared for example to α_{QED}) this third order effect still has a significant impact on the numerical results.

The quantitative investigation of this scale dependence inherent in equation (2) shows that it only depends on the magnitude of the second order term relative to the first order term. There are therefore two possibilities to formally eliminate the sensitivity to the choice of μ:

- The higher order term can be almost cancelled at $\mu \approx \sqrt{s}$ if one considers differences of variables with similar next to leading order terms. Examples are the difference of the heavy and light jet masses and the energy-energy correlation asymmetry.
- The normally large and positive term B can be compensated by the term $2\pi b_0 \ln(\mu^2/s)$ if the logarithm becomes large and negative, i.e. if the scale is chosen to be $\mu^2 = f \cdot s$

with $f \ll 1$. Several theoretical prescriptions for scale optimization have been given in the literature, all tending to at least partially cancel the next to leading order term and therefore generally leading to very small scales [10]. Very small scales contradict, on the other hand the naive expectation that the perturbative series can only be well-behaved for f close to 1.

However, the smallness of the second order term does not guarantee that the third order term is negligible. We prefer to determine the value $\alpha_s(M_Z^2)$ using the QCD prediction for $f = 1$ and to use the Lund Matrix Element (ME) [7] model tuned at $f = 1$ to empirically correct for fragmentation effects and treat the scale dependence separately. Part of the impact of higher order corrections can be studied by means of shower Monte Carlo models which include higher order QCD effects in the framework of the leading-logarithm approximation. A reliable improvement of these systematic uncertaintiues is more likely to result from a complete third order QCD calculation than from sophisticated choices of μ.

Some other experiments have chosen to study the result for $\alpha_s(M_Z^2)$ using a version of the Lund ME model tuned at $f = 0.002$ [11]. In this case the model is able to better describe event shape distributions even in regions where second order perturbation theory breaks down, e.g., the y_3 distribution in the region $y_3 < 0.05$. In the fitting ranges used in this paper there is no improvement of the fit quality when going to $f = 0.002$. In order to permit to translate our results for $\alpha_s(M_Z^2)$ to different choices for the renormalization scale we give an explicit parameterization of the shift in $\alpha_s(M_Z^2)$ with f for every event shape variable. All results quoted here refer to the choice $f = 0.25$.

4. Model Calculations

The transition from the second order to the final hadronic level has been investigated using the Lund Matrix Element (ME) [7] and the Lund $O(\alpha_s)$ Parton Shower (PS) model [5] as implemented in the program JETSET version 7.2. In both types of models one starts with a system of partons generated according to perturbative QCD. In the shower model the initial quark-antiquark pair evolves into a system of quarks and gluons according to the leading-logarithm approximation [12,8]. Successive branchings of the type $q \to qg$, $g \to gg$ and $g \to q\bar{q}$ are repeated until the invariant mass of the resulting partons falls below a specified cut-off of $O(1\ GeV)$. The final conversion of partons into colour neutral hadrons is simulated using the string fragmentation scheme. In the ME approach the perturbative state hadronizes directly according to the Lund string fragmentation model.

Specifically we considered the following models, all of which were tuned to give a good description of hadronic Z^0 decays as measured experimentally [9]:

(1) Lund $O(\alpha_s^2)$ ME model, JETSET version 7.2, based on ERT matrix elements evaluated for a renormalization scale $\mu^2 = M_Z^2$.

(2) Lund $O(\alpha_s^2)$ ME model, JETSET version 7.2, based on ERT matrix elements evaluated for a renormalization scale $\mu^2 = 0.002 \cdot M_Z^2$.
By enhancing the four-jet cross section this modification of the matrix element model provides a better description of the data than the previous one [13,14].

(3) Lund PS model with the parton level defined at an intermediate level in the shower history where the parton off-shellness falls below a cut-off scale of 13 GeV.

The value of 13 GeV was chosen in order to have the same average parton multiplicity as given by the matrix element model with the renormalization scale $\mu^2 = M_Z^2$ (model 1).

(4) Lund PS model with the parton level defined at an intermediate cut-off scale of 7.2 GeV. Here the cut-off scale was chosen such that the average parton multiplicity is four, which can be viewed as the limiting case of a second order matrix element model with the infrared cut-off pushed down to zero.

In the ME models (1) and (2), the relative probabilities for two-, three-, and four-parton final states are given by integrating the $O(\alpha_s^2)$ QCD formulae over a region of phase space limited by the infrared cut-off parameter $y_{min} = m_{ij}^2/s = 0.01$, the minimum scaled invariant mass squared of any two partons i and j. For the QCD formulae used to determine α_s there is no such cut-off. Therefore the parton level distributions from Lund ME do not exactly correspond to the theoretical predictions [2], even though both are based on the same QCD matrix elements. More precisely, since the infrared cut-off increases the average invariant mass of any two-parton system, the matrix elements effectively are evaluated at a higher than the nominal renormalization scale $\mu^2 = M_Z^2$ (in model 1) and $\mu^2 = 0.002 \cdot M_Z^2$ (in model 2), respectively, thereby bracketing a choice of $\mu^2 = M_Z^2$ in equation 2. The intermediate mass scales in the parton shower models (models 3 and 4) were chosen such that the intermediate level represents approximately the result of a second order QCD calculation. The ambiguity in the cut-off scale that defines this "second order" level thereby is related to the arbitrariness of the renormalization scale μ in perturbative QCD, the higher cut-off (model 3) corresponding to a larger scale μ and the lower cut-off (model 4) to a smaller scale, respectively.

In order to separate the effects of perturbative higher orders and the final hadronization step, the effect of the hadronization alone was studied for two models:

(5) Lund PS model with "parton level" defined at the end of the shower, and hadronization according to the Lund string fragmentation model.

(6) HERWIG model. A parton shower similar to that of the Lund PS is generated with "parton level" defined at the end of the shower development. The hadronization is carried out according to a cluster model.

Since both these models employ very similar algorithms to simulate perturbative higher orders, but use very different fragmentation schemes, the differences between the two give an indication of the uncertainty due to the hadronization process.

5. Experimental Results

Corrected values for α_s were determined with transition probabilities p_{ij} from all models under consideration. In addition an uncorrected value α_s^{uncorr} was fitted, setting $p_{ij} = \delta_{ij}$, i.e. pretending that the measured distributions are undistorted with respect to the second order parton level distributions. Except for oblateness the theoretical predictions fit the data well. The results translated to a renormalization scale $\mu = M_Z/2$ are given in table 1. The uncorrected value $\alpha_s(M_Z^2)^{uncorr}$ is listed together with the range of values $\alpha_s(M_Z^2)^{hadr}$ obtained when correcting for hadronization only (models 5 and 6) and the range $\alpha_s(M_Z^2)^{corr}$ obtained after correction for hadronization plus perturbative higher orders (models 1 – 4).

Variable	Fit Interval	$\alpha_s(M_Z^2)^{uncorr}$	$\alpha_s(M_Z^2)^{hadr}$	$\alpha_s(M_Z^2)^{corr}$
Thrust	0.70 - 0.90	0.140 ± 0.002	$0.130 - 0.135$	$0.106 - 0.123$
Oblateness	0.10 - 0.40	0.090 ± 0.001	$0.125 - 0.142$	$0.150 - 0.204$
C	0.32 - 0.60	0.139 ± 0.002	$0.119 - 0.132$	$0.095 - 0.117$
$M_{H,T}^2/s$	0.10 - 0.20	0.130 ± 0.002	$0.123 - 0.138$	$0.124 - 0.146$
$M_{D,T}^2/s$	0.10 - 0.20	0.100 ± 0.002	$0.113 - 0.127$	$0.128 - 0.142$
y_3	0.10 - 0.20	0.119 ± 0.002	$0.120 - 0.124$	$0.114 - 0.123$

Table 1: Fit intervals, uncorrected values for $\alpha_s(M_Z^2)$ (using $p_{ij} = \delta_{ij}$) and ranges obtained when correcting only for hadronization (p_{ij} from models 5 and 6) or for both hadronization and perturbative higher orders (p_{ij} from models 1 to 4). The renormalization scale $\mu = M_Z/2$ applies throughout.

From table 1 it is clear that the most robust variable for the measurement of α_s is y_3, because the corrections have the least influence on the result. One also sees that the corrected values all are consistent with each other. The remarkable stability of y_3 can be understood as a result of the E_0 clustering algorithm together with the JADE metric for y_{ij} where mass effects are systematically ignored in a consistent way both on parton and on hadron level. Alternative recombination schemes, the E and p-scheme as defined in reference [2], constituting alternative event shape variables with different theoretical predictions, have been tried but were found to be subject to larger theoretical uncertainties. We will therefore retain only the results from the differential 2-jet rate based on the most stable recombination algorithm.

Comparison of the uncorrected value for α_s, first with the one corrected for hadronization effects, and then with the final result that includes also the correction for higher-than-second order effects permits an evaluation of the impact of perturbative higher orders and of non-perturbative effects on the different event-shape variables. Thrust for instance is only weakly affected by hadronization process, but significantly biased by perturbative higher orders. Oblateness on the other hand is very sensitive to effects of both higher orders and hadronization. The C-parameter is found to behave similarly to thrust, albeit with slightly larger sensitivity to the theoretical uncertainties. Finally one finds that both $M_{H,T}$ and $M_{D,T}$ are moderately dependent on higher orders and hadronization.

The results given in table 1 correspond to a renormalization scale in equation 2 set to $\mu = M_Z/2$. The small shifts in $\alpha_s(M_Z^2)$ induced by changing this formal parameter of the theory has been determined by fitting the uncorrected second order QCD prediction to the data for various values of μ. These shifts have been parameterized in the form

$$\alpha_s(f) - \alpha_s(f_0) \;=\; (c_1 + 2c_2 \ln f_0) \cdot \ln \frac{f}{f_0} + c_2 \ln^2 \frac{f}{f_0}.$$

with $f = \mu^2/M_Z^2$. The results for the different event-shape variables are summarized in table 2. The first column gives the nominal results for $\alpha_s(M_Z^2)$ obtained with the Lund ME (model 1) correction, which is expected to be the most reliable correction from parton to hadron level since it contains the same QCD matrix elements at the same renormalization scale as used in the fitting procedure. The first error given is the statistical and systematic error of the experiment combined in quadrature, the second the theoretical uncertainty due to higher-than-second order effects, which dominates in all cases. The latter was estimated by the maximum discrepancy between the corrected value based on model (1) and the range of values given in table 1. As this is a rough estimate of the error, it is conservatively quoted as being symmetric. The second and

third columns contain the coefficients of our parameterization of the scale dependence $\Delta\alpha_s(f)$ and the last column a lower limit for the scale parameter f for which the parameterization is still less than one (statistical) standard deviation away from the fitted result.

Distribution	$\alpha_s(M_Z^2)\,, f = 0.25$	c_1	c_2	f_{min}
Thrust	$0.119 \pm 0.004 \pm 0.013$	0.0093	0.00051	0.001
Oblateness	$0.186 \pm 0.003 \pm 0.036$	0.0003	0.00133	0.040
C	$0.112 \pm 0.004 \pm 0.017$	0.0089	0.00051	0.001
$M_{H,T}^2/s$	$0.136 \pm 0.004 \pm 0.012$	0.0063	0.00052	0.003
$M_{D,T}^2/s$	$0.142 \pm 0.004 \pm 0.014$	0.0025	0.00054	0.004
y_3	$0.121 \pm 0.004 \pm 0.007$	0.0053	0.00037	0.001

Table 2: Results for $\alpha_s(M_Z^2)$ and coefficients of a parameterization for the change $\alpha_s(f) - \alpha_s(f_0) = (c_1 + 2c_2 \ln f_0) \cdot \ln(f/f_0) + c_2 \ln^2(f/f_0)$ found by fitting $\alpha_s(\mu^2 = f \cdot M_Z^2)$ and evolving this to $\alpha_s(M_Z^2)$. The last column gives a lower limit for the scale parameter f where the parameterization is still within the statistical error of the fitted result.

Finally, we choose the differential 2-jet rate based on the E_0- algorithm for the best determination of α_s, because this variable has the smallest theoretical uncertainties. Since the choice of the renormalization scale is arbitrary, we consider conservatively all scales from $\mu = M_Z$ down to the b-quark mass. Using the information in table 2, the result for the central value $\mu = M_Z/2$ is found to be

$$\alpha_s(M_Z^2) = 0.121 \pm 0.002 \pm 0.003 \pm 0.007$$

where the errors are the statistical error, experimental systematics and the theoretical uncertainties due to perturbative higher orders and hadronization effects. The dependence on μ changes the result in addition by $^{+0.007}_{-0.012}$.

Figure 3 shows the measured y_3 distribution compared to the fitted theoretical predictions for QCD only and also QCD folded with the Lund-ME transition probabilities. The fitted values of α_s are 0.119 for pure second order QCD and 0.121 after the Lund-ME correction. The good agreement between data and theory extends well outside the restricted range chosen for the fit: the result clearly is insensitive to the choice of this range.

These results are in good agreement with those obtained by Mark II [15] and by the other LEP experiments [11] if translated to the respective choices of renormalization scale. They also agree with measurements by OPAL and DELPHI based on energy-energy correlations [16].

6. Summary

We have measured the strong coupling constant $\alpha_s(M_Z^2)$ from global event-shape variables in hadronic Z^0 decays. Within their theoretical uncertainties the shape variables studied yield consistent results. The measurement with the smallest theoretical error is obtained from the differential 2-jet rate measured with the E_0-clustering algorithm:

$$\alpha_s(M_Z^2) = 0.121 \pm 0.002(stat.) \pm 0.003(sys.) \pm 0.007(theo.)$$

for $\mu = M_Z/2$. The dependence on the choice of the renormalization scale can be parameterized as

$$\alpha_s(M_Z^2, f) - \alpha_s(M_Z^2, f = 0.25) \quad = \quad 0.0043 \cdot \ln(4f) + 0.00037 \cdot \ln^2(4f).$$

This corresponds to an additional error of $^{+0.007}_{-0.012}$ if μ is allowed to vary between M_Z and the b-quark mass.

Acknowledgement

We would like to thank our colleagues of the LEP division for the excellent performance of the LEP storage ring. Thanks are also due to engineers and technical personnel at all collaborating institutions for their support in constructing and maintaining ALEPH . Those of us from non-member states thank CERN for its hospitality.

Figure Captions

Figure 1: Distribution of y_3 observed on hadron level versus y_3 distribution on parton level in the Lund second order matrix element model. The gap due to the infrared cut-off $y_{min} = 0.01$ is clearly visible. The dotted lines indicate the region used for the fit of α_s, chosen such that it is unaffected by the infrared cut-off.

Figure 2: Lund ME (model 1) predictions for the ratio of the parton level and hadron level distributions of y_3 (part a) and Oblateness, O, (part b) as well as smearing for both variables when going from the partonic to the hadronic level for $0.1 \leq y_{3h} \leq 0.2$ (part c) and $0.1 \leq O_h \leq 0.4$ (part d).

Figure 3: Measured y_3 distribution corrected for detector effects, decays and missing neutrals compared to the second order QCD prediction with scale fixed to $\mu = M_Z/2$. The solid line represents the second order predictions convoluted with the smearing information from the Lund matrix element model and the dashed line the fit without corrections for perturbative higher orders and hadronization.

References

[1] A. Ali and F. Barreiro *Jets in e^+e^- Annihilations and QCD* , in *Advanced Series on Directions in HEP Vol.1,* eds. A. Ali and P. Söding, World Scientific (1988), p. 611 ff.

[2] Z. Kunszt, P. Nason, G. Marchesini and B.R. Webber, *QCD* , in *Proceedings of the Workshop on Z Physics at LEP,* eds. G. Altarelli, R. Kleiss and C. Verzegnassi, CERN Report 89-08, p. 373 ff.

[3] *ALEPH – a Detector for Electron-Positron Annihilation at LEP,* Nucl. Instr. Meth. **A294** (1990) 121.

[4] W. Bartel et al., JADE Collaboration, Z. Phys. C **33** (1986) 23;
S. Bethke et al., JADE Collaboration, Phys. Lett. **B213** (1988) 235.

[5] M. Bengtsson and T. Sjöstrand, Phys. Lett. **185B** (1987) 435.

[6] R.K. Ellis, D.A. Ross and A.E. Terrano, Nucl. Phys. **B178**(1981)421.

[7] T. Sjöstrand and M. Bengtsson, Comput. Phys. Commun. **43** (1987) 367.

[8] G. Marchesini and B.Webber, Cavendish-HEP-88/7 (1988);
G. Marchesini and B. Webber, Nucl. Phys. **B310** (1988) 461;
I. Knowles, Nucl. Phys. **B310** (1988) 571.

[9] ALEPH Collaboration, *Properties of Hadronic Z Decays and Test of QCD Generators*, to be published

[10] P.M. Stevenson, Phys. Rev. **D16** (1981) 2916;
S.J. Brodsky, G.P. Lepage and P.B. Mackenzie, Phys. Rev. **D28** (1983) 228;
G. Grunberg, Phys. Lett. **B95** (1980) 70.

[11] M.Z. Akrawy et al., OPAL Collaboration, Phys. Lett. **B235** (1990) 389;
M.Z. Akrawy et al., OPAL Collaboration, CERN-PPE/90-143;
P. Abreu et al., DELPHI Collaboration, CERN-EP/90-89;
B. Adeva et al., L3 Collaboration, Phys. Lett. **B248** (1990) 462.

[12] Yu.L. Dokshitzer, V.A. Khoze, S.I. Troyan and A.H. Mueller, Rev. Mod. Phys. **60** (1988) 373;
C.P. Fong and B.R. Webber, Cavendish-HEP-90/2.

[13] S. Bethke, Z. Phys. C **43** (1989) 331.

[14] G. Kramer and B. Lampe, J. Math. Phys. **28** (1987) 945; Z. Phys. C **34** (1987) 497; **39** (1988) 101.

[15] S. Komamiya et al., Mark II Collaboration, Phys. Rev. Lett. **64** (1990) 987.

[16] M.Z. Akrawy et al., OPAL Collaboration, CERN-PPE/90-121;
P. Abreu et al., DELPHI Collaboration, CERN-PPE/90-122.

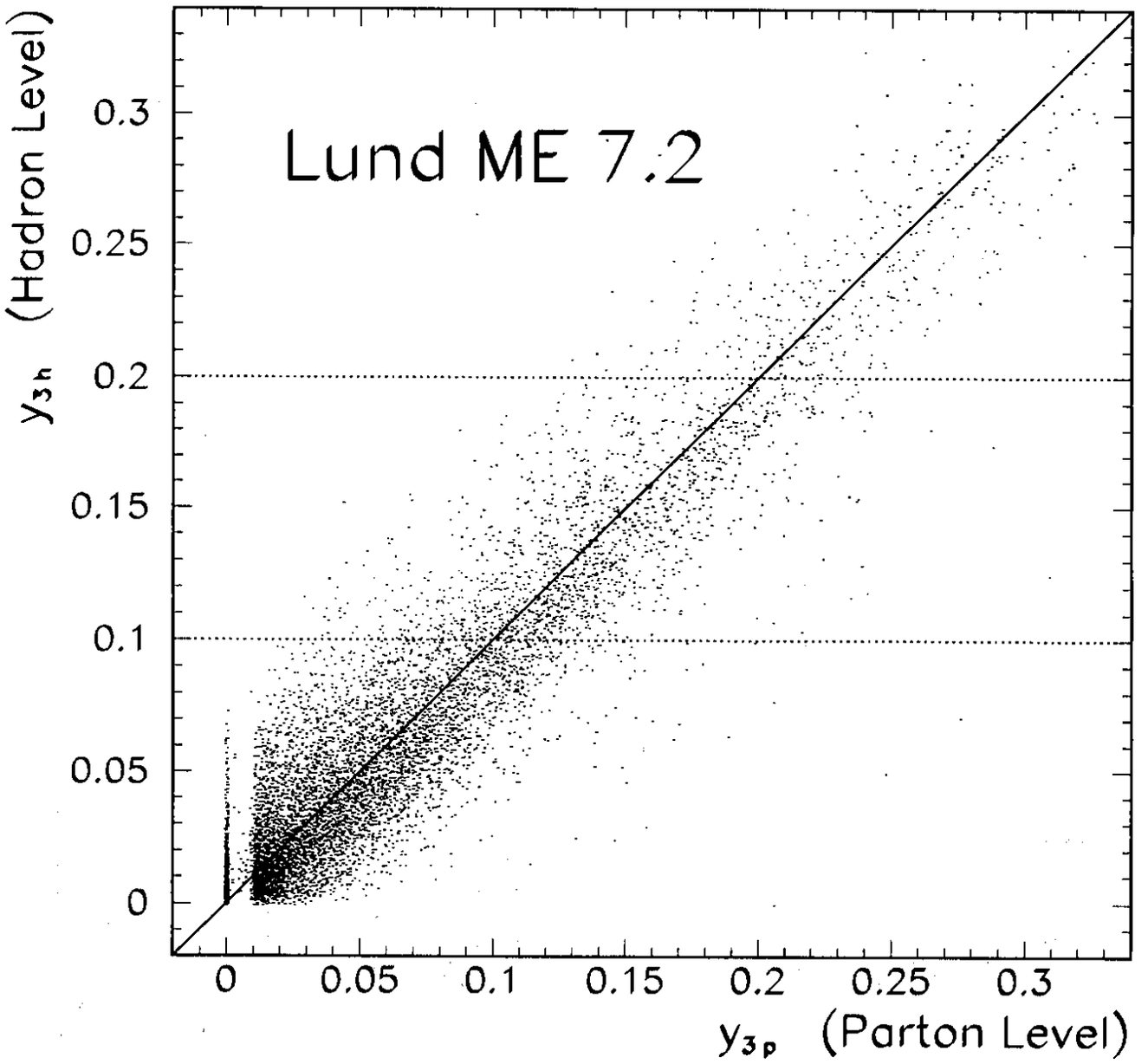
Lund ME 7.2
y_{3h} (Hadron Level)
y_{3p} (Parton Level)
0
0.05
0.1
0.15
0.2
0.25
0.3

Figure 1:

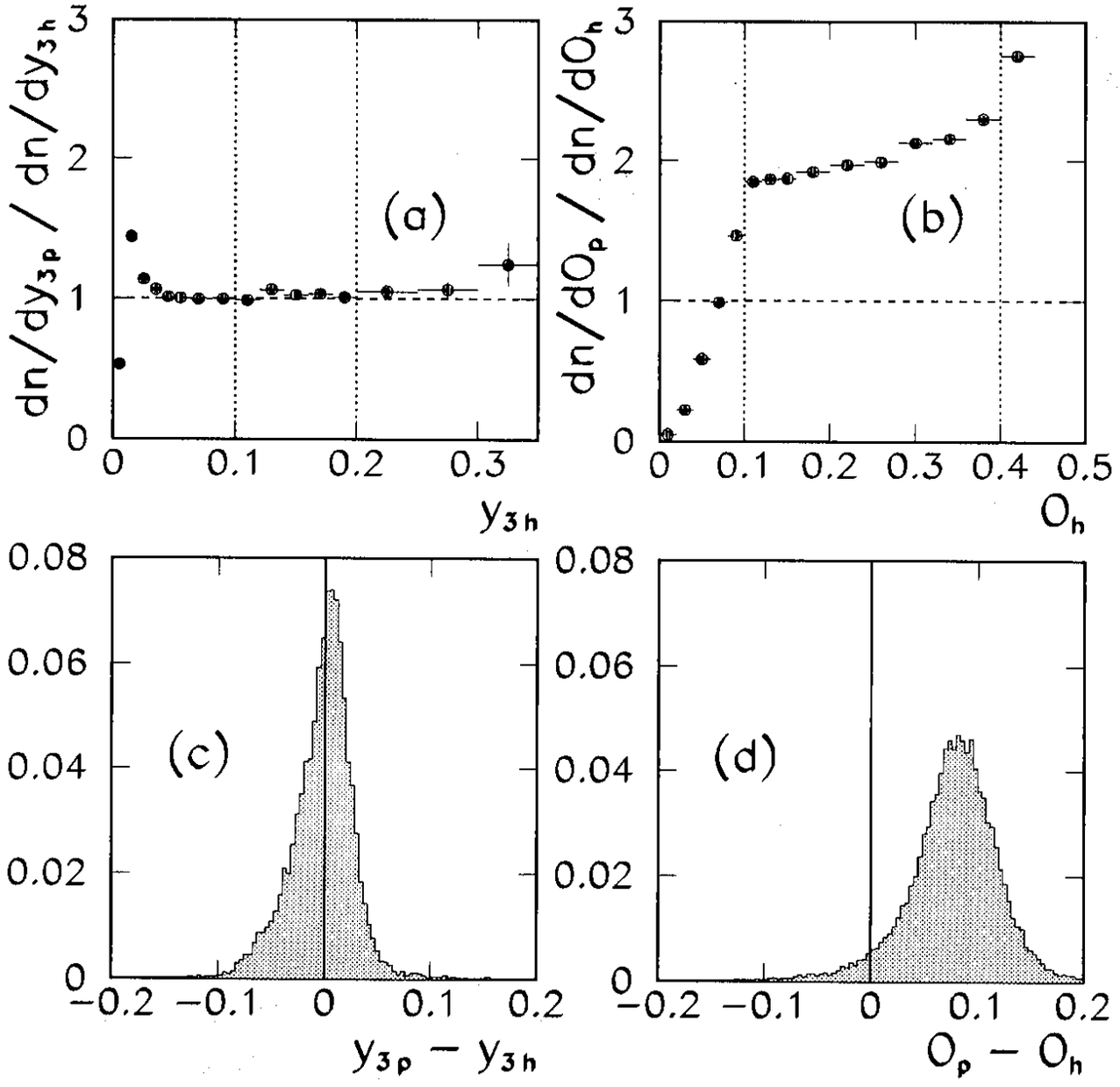

Figure 2:

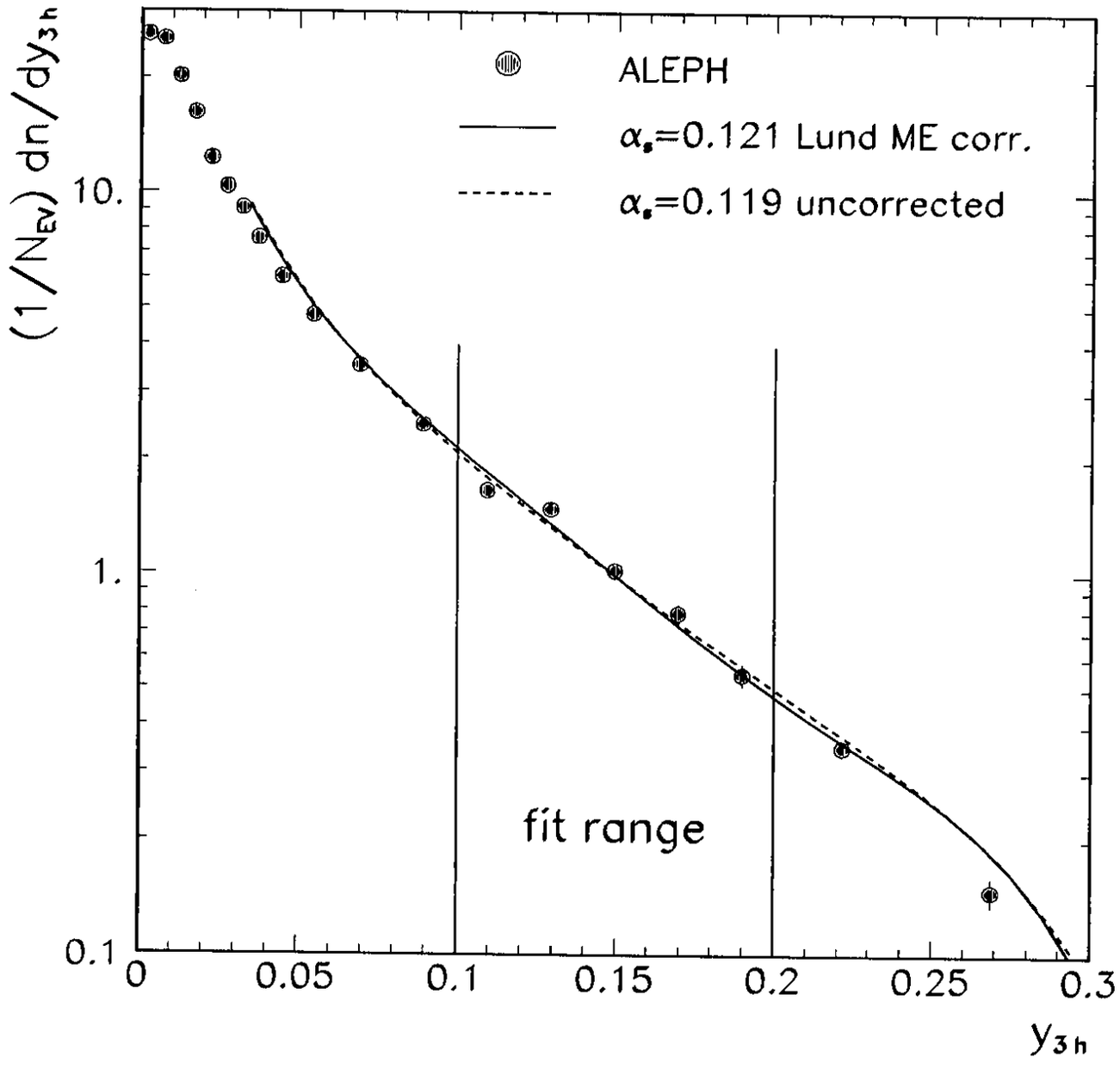

Figure 3:

Imprimé au CERN. Prix : 0.35 Fr.